

# Supplemental Figures

## Figure S1

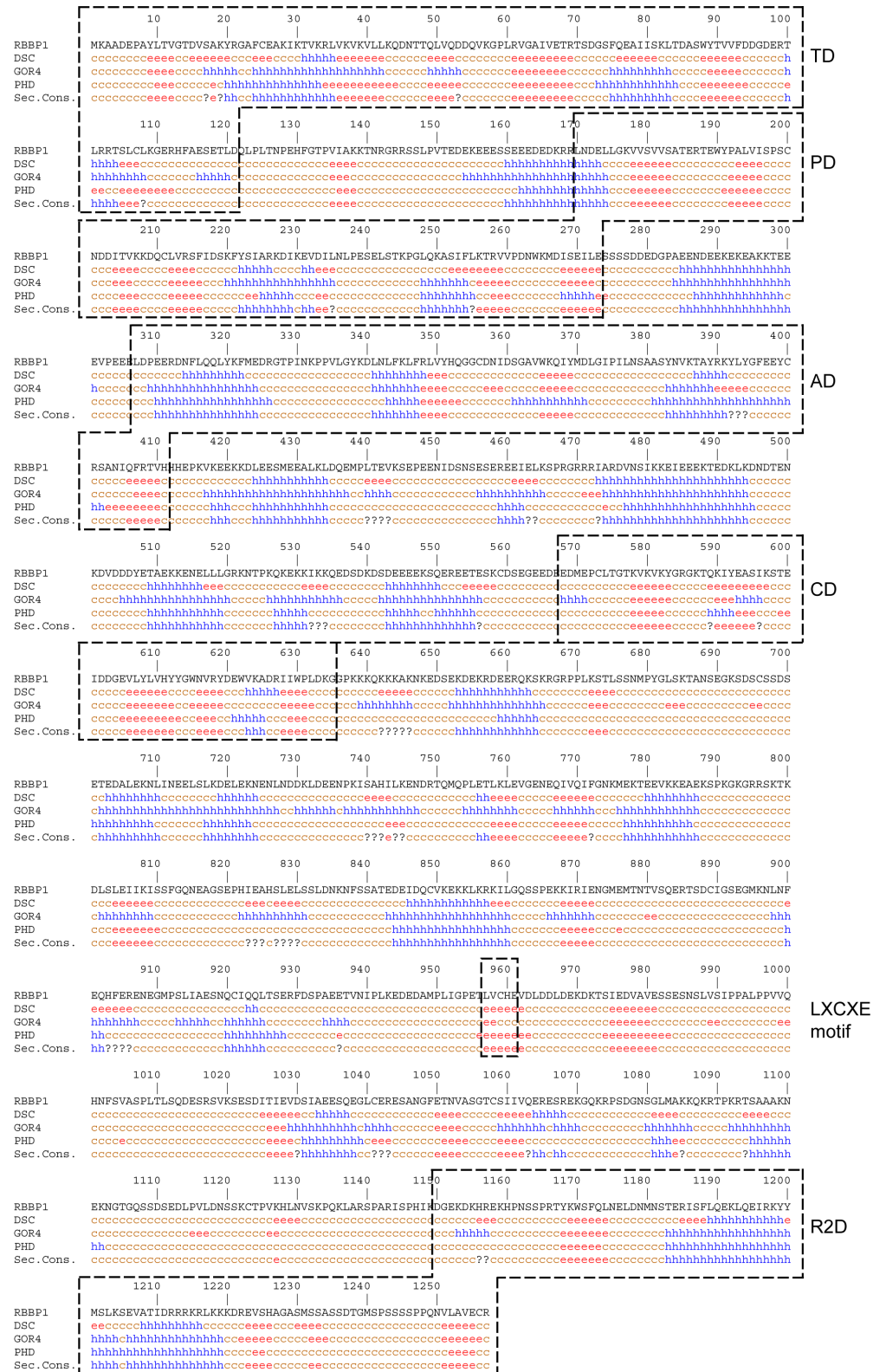


Figure S1. The consensus secondary structure prediction of RBBP1 using the NPS@ server [1]. Combining this prediction and the following two figures, five ordered domains were defined and are indicated by dashed lines. The LXCXE motif, which is the pRb binding site, is also indicated.

Figure S2

Red: Disordered residues Black: Ordered residues

1	<b>MKAADEPAYL</b>	TVGTDVSAKY	RGAFCEAKIK	TVKRLVKVKV	LLKQDNTTQL	TD
51	VQDDQVKGPL	RVGAIVETRT	SDGSFQEAI	SKLTDASWYT	VVFDDGDERT	
101	LRRTSLCLK <b>G</b>	<b>ERHFAESETL</b>	DQLPLTNPEH	FGT <b>PVIAKKT</b>	<b>NRGRRSSLPV</b>	PD
151	<b>TEDEKEEES</b>	<b>EEDEDEKRRL</b>	NDELLGKVVS	VVSATERTEW	YPALVISPSC	
201	NDDITVKKDQ	CLVRSFIDSK	FYSIARKDIK	EV <b>DILNLPES</b>	<b>ELSTKPGLOK</b>	AD
251	ASIFLKTRVV	PDNWKMDISE	<b>ILES</b> SSSDDE	<b>DGPAEENDEE</b>	<b>KEKEAKKTEE</b>	
301	<b>EVPEEELDPE</b>	ERDNFLQQLY	KFMEDRGTP	NKPPVLGYKD	LNLFKLFRLV	AD
351	YHQGGCDNID	SGAVWKQIYM	DLGIPILNSA	ASYNVKTAYR	KYLYGFEEYC	
401	RSANIQ <b>FRTV</b>	<b>HHHEPKVKEE</b>	<b>KKDLEESMEE</b>	<b>ALKLDQEMPL</b>	<b>TEVKSEPEEN</b>	CD
451	<b>IDSNSESERE</b>	<b>EIELKSPRGR</b>	<b>RRIARDVNSI</b>	<b>KKEIEEEKTE</b>	<b>DKLKDNDTEN</b>	
501	<b>KDVDDDYETA</b>	<b>EKKENELLG</b>	<b>RKNTPKQKEK</b>	<b>KIKKQEDSDK</b>	<b>DSDEEEESQ</b>	CD
551	<b>EREETESKCD</b>	<b>SEGEED</b> EDM	<b>EPCLTGT</b> KVK	VKYGR <b>RGKTQK</b>	<b>IYEASIKSTE</b>	
601	IDDGEVLYLV	HYYGWNVRYD	EWVKADRIW	PLDK <b>GGPKKK</b>	<b>QKKKAKNKED</b>	LXCXE motif
651	<b>SEKDEKRDEE</b>	<b>RQSKRGRPP</b>	<b>LKSTLSSNMP</b>	<b>YGLSKTANSE</b>	<b>GKSDSCSSDS</b>	
701	<b>ETEDALEKNL</b>	<b>INEELSLKDE</b>	<b>LEKNENLNDD</b>	<b>KLDEENPKIS</b>	<b>AHILKENDRT</b>	LXCXE motif
751	<b>QMOPLETLKL</b>	EVGENEQIVQ	IFGN <b>KMEKTE</b>	<b>EVKKEAEKSP</b>	<b>KGKGRRSKTK</b>	
801	<b>DLSLEIIKIS</b>	<b>SFGQNEAGSE</b>	<b>PHIEAHSLEL</b>	<b>SSLDNKNFSS</b>	<b>ATEDEIDQCV</b>	LXCXE motif
851	<b>KEKKLKRKIL</b>	<b>GQSSPEKKIR</b>	<b>IENGMEMTNT</b>	<b>VSQERTSDCI</b>	<b>GSEGKMKLNF</b>	
901	<b>EQHFERENEG</b>	<b>MPSLIAESNQ</b>	<b>CIQQLT</b> SERF	<b>DSPAETVNI</b>	<b>PLKEDEDAMP</b>	LXCXE motif
951	LIGPETLVCH	EV <b>DLDDLDEK</b>	<b>DKTSIEDVAV</b>	<b>ESSESNSLVS</b>	<b>IPPALPPVVQ</b>	
1001	<b>HNFVASPLT</b>	<b>LSQDESRSVK</b>	<b>SESDITIEVD</b>	<b>SIAEESQEGL</b>	<b>CERESANGFE</b>	LXCXE motif
1051	<b>TNVASGTCSI</b>	<b>IVQERESREK</b>	<b>GQKRPSDGNS</b>	<b>GLMAKKQKRT</b>	<b>PKRTSAAAKN</b>	
1101	<b>EKNGTGQSSD</b>	<b>SEDLPVLDNS</b>	<b>SKCTPVKHLN</b>	<b>VSKPQKLARS</b>	<b>PARISPHIKD</b>	R2D
1151	<b>GEKDKHREKH</b>	<b>PNSSPRT</b> YKW	SFQLNELDNM	NSTERISFLQ	EKLQEIRKYY	
1201	MSLKSEV <b>ATI</b>	<b>DRRRKRLKKK</b>	<b>DREVS</b> HAGAS	<b>MSSAS</b> SDTGM	<b>SPSSSSPPQN</b>	R2D
1251	<b>VLAVECR</b>					

Figure S2. The result of protein disorder prediction of RBBP1 using the PrDOS server [2].

Figure S3

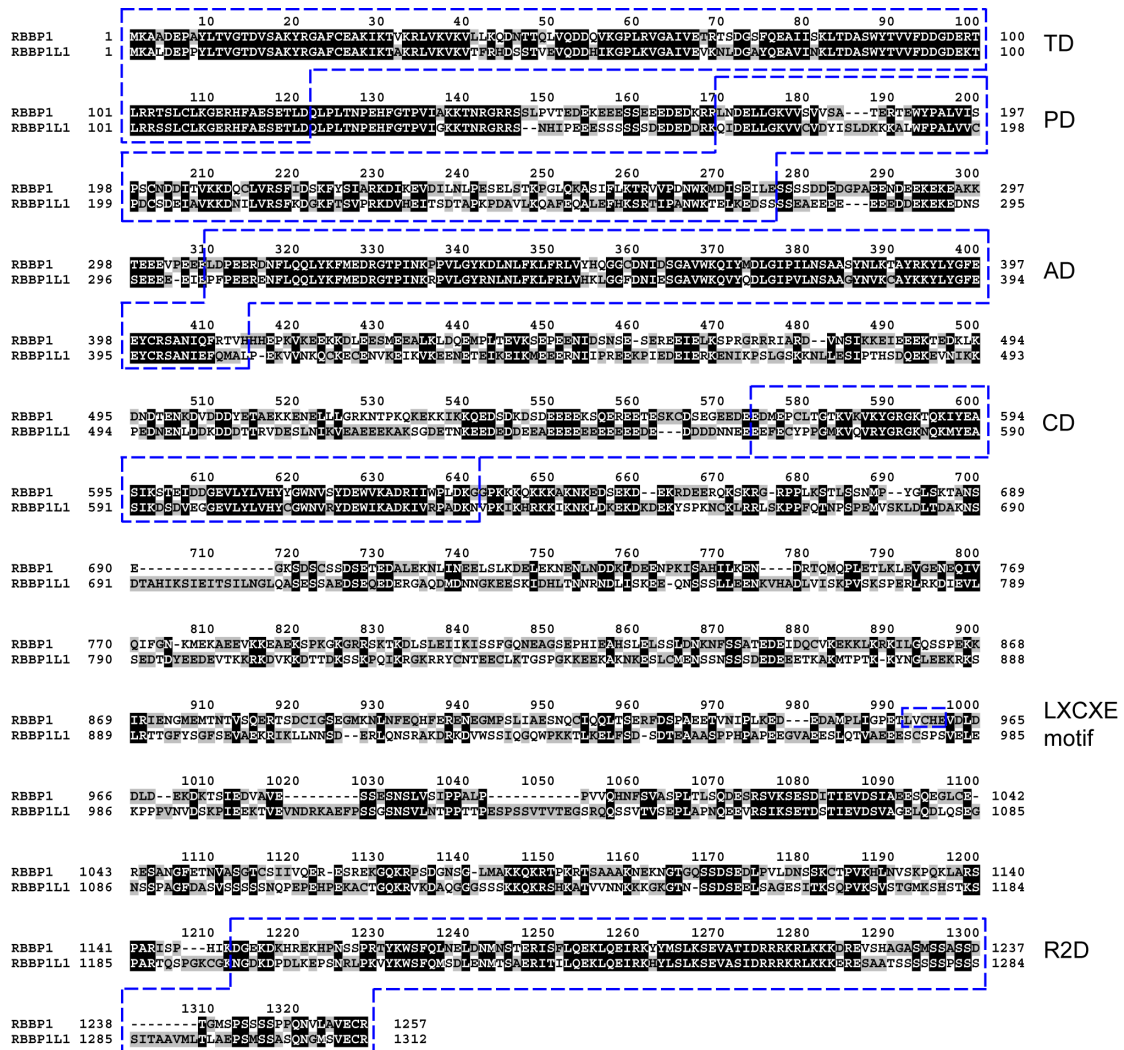


Figure S3. Sequence alignment of RBBP1 and RBBP1L1. The sequence identity between RBBP1 and RBBP1L1 of the domains is 80% for TD, 44% for PD, 78% for AD, 65% for CD, 61% for R2D, and the identity of other regions is less than 29%.

Figure S4.

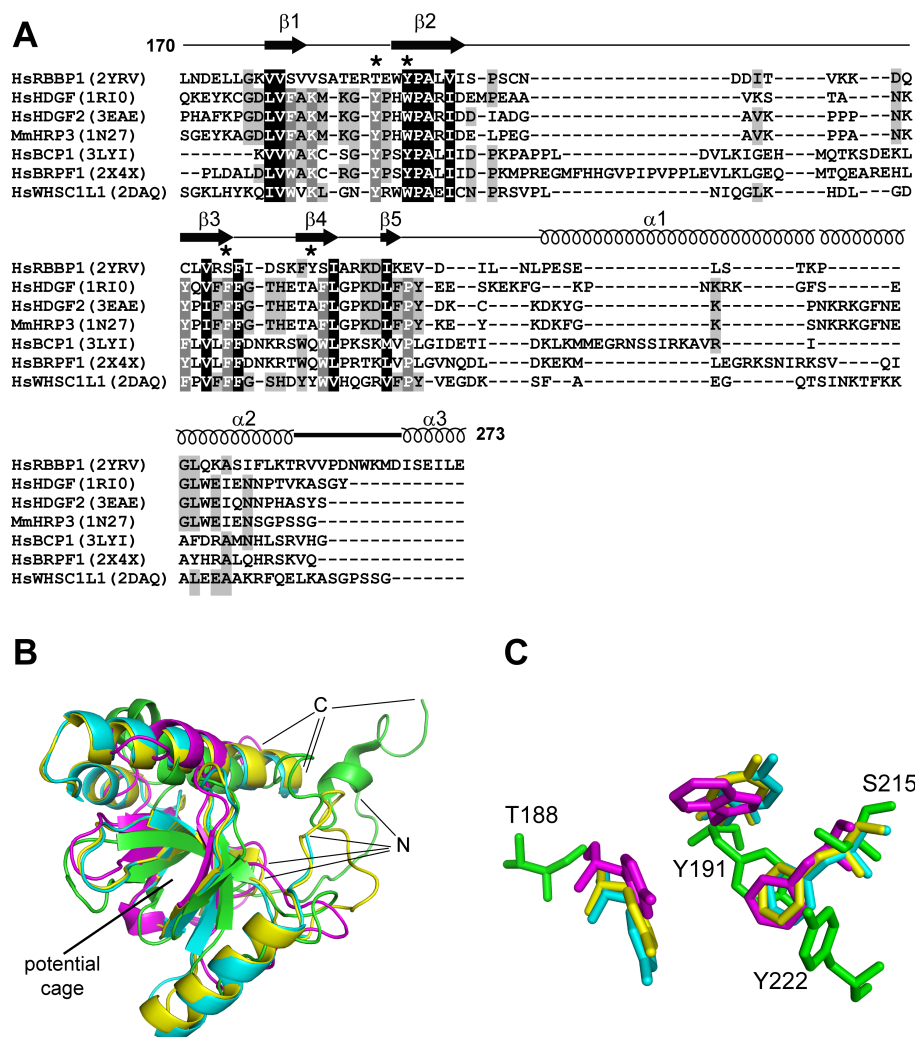


Figure S4. Structural comparison of RBBP1 PD with other PWWP domains. PWWP domains were named originally after the Pro-Trp-Trp-Pro motif in the domain, but the motif is not conserved in all PWWP domain proteins [3], such as the Brpf1 PWWP domain [4]. The residues corresponding to the motif Pro-Trp-Trp-Pro in PWWP domains are Glu<sup>189</sup>-Trp<sup>190</sup>-Tyr<sup>191</sup>-Pro<sup>192</sup> in the RBBP1 PD. (A) Structure-based sequence alignment of RBBP1 PD with other PWWP domains for which structures are available. The structure-based alignments were made using SSM [5]. The PDB accession codes used in the alignment are shown in parentheses. Residues forming an aromatic cage and structurally-corresponding residues are indicated by stars. (B) Superimposition of PDs of RBBP1 (green, PDB 2YRV), Hrp3 (magenta, PDB 1N27), Bcp1 (cyan, PDB 3LYI) Brpf1 (yellow, PDB 2X4X). (C) The residues forming aromatic cages and structurally-corresponding residues in the structure superimposition. The colors are same as those in (B). Two of the three residues involved in forming the aromatic cages in other PWWP domains are not conserved in the RBBP1 PD. However, an additional aromatic residue Tyr<sup>222</sup> is present around the expected position of the aromatic cage in the RBBP1 PD. Therefore, whether or not the RBBP1 PD is able to recognize methylated histone tails could not be determined from inspection of the structure alone.

Figure S5.

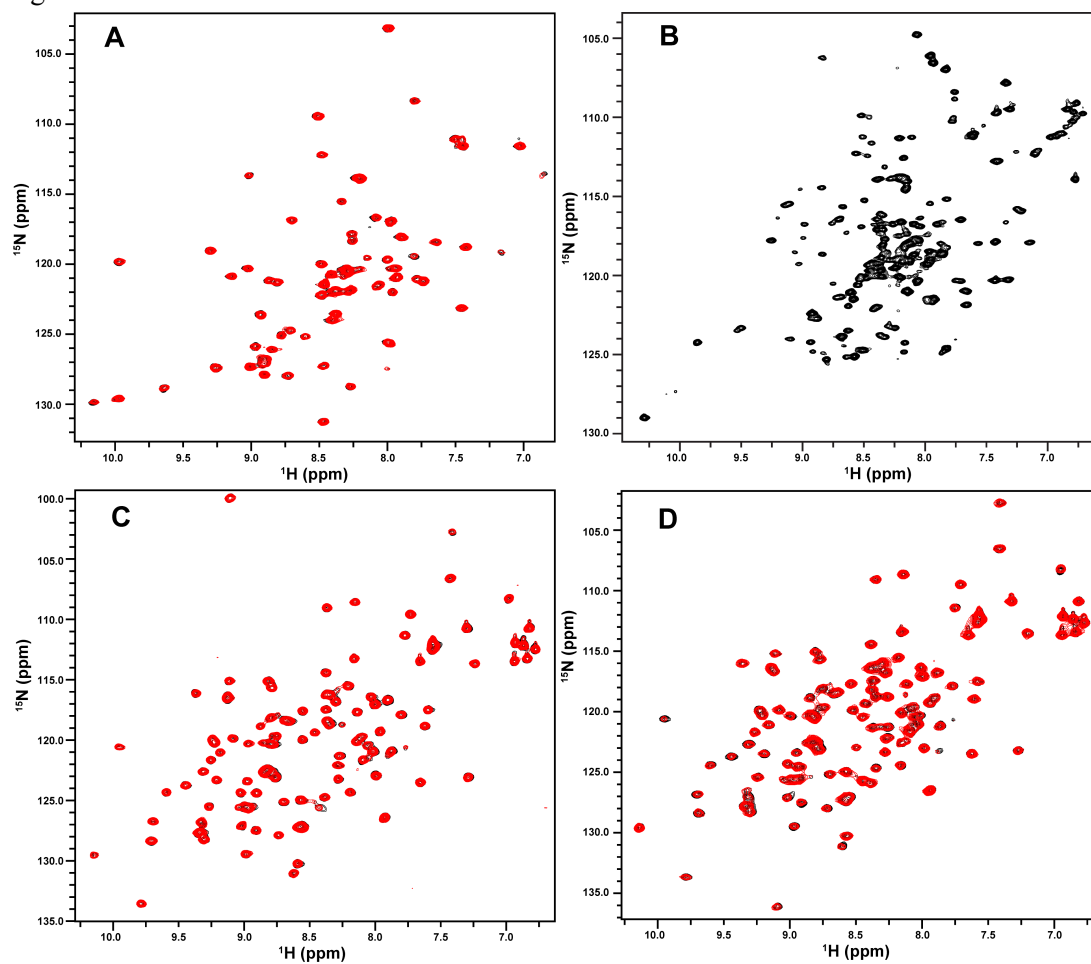


Figure S5. RBBP1 CD, PD and TD are independent domains and do not interact with each other. (A)  $^1\text{H}$ - $^{15}\text{N}$  HSQC spectra of RBBP1 CD in the absence (black) and presence (red) of RBP1 PD. (B)  $^1\text{H}$ - $^{15}\text{N}$  HSQC spectrum of RBBP1 PD. (C)  $^1\text{H}$ - $^{15}\text{N}$  HSQC spectra of RBBP1 TD in the absence (black) and presence (red) of RBBP1 CD. (D)  $^1\text{H}$ - $^{15}\text{N}$  HSQC spectra of RBBP1 CD in the absence (black) and presence (red) of RBBP1 TD.

Figure S6

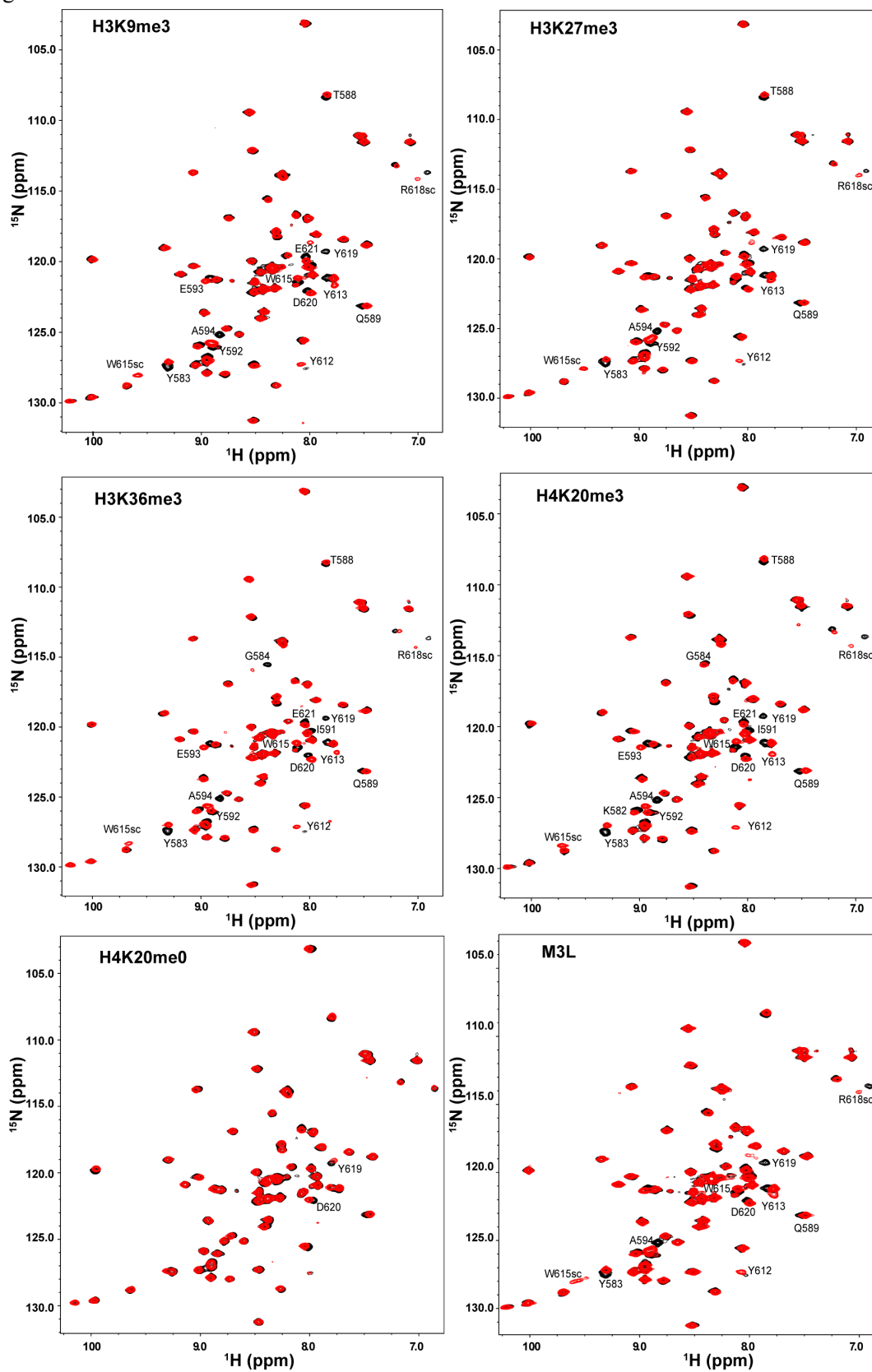


Figure S6. The overlaid  $^1\text{H}$ - $^{15}\text{N}$  HSQC spectra of RBBP1 CD in the titration with H3K9me3 (1:12), H3K27me3 (1:12), H3K36me3 (1:12), H4K20me3 (1:12), M3L (1:12) and H4K20me0 (1:18).

Figure S7.

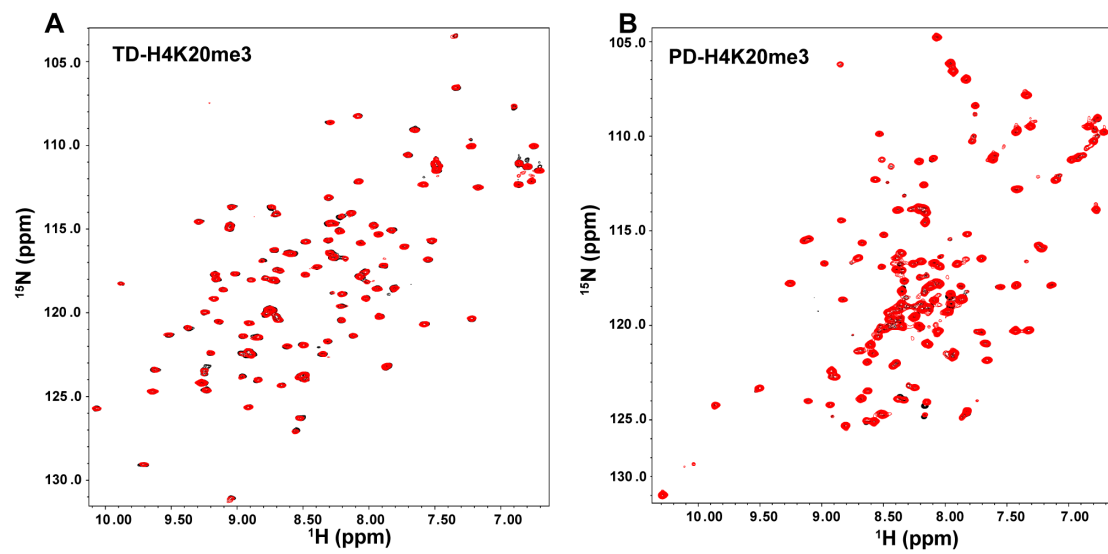


Figure S7. The overlaid  $^1\text{H}$ - $^{15}\text{N}$  HSQC spectra of RBBP1 TD (A) and PD (B) in the titration with H4K20me3 (1:7 for TD and 1:6 for PD). The spectra of RBBP1 TD and PD titrated with other peptides were the same and are not shown.



Figure S8.

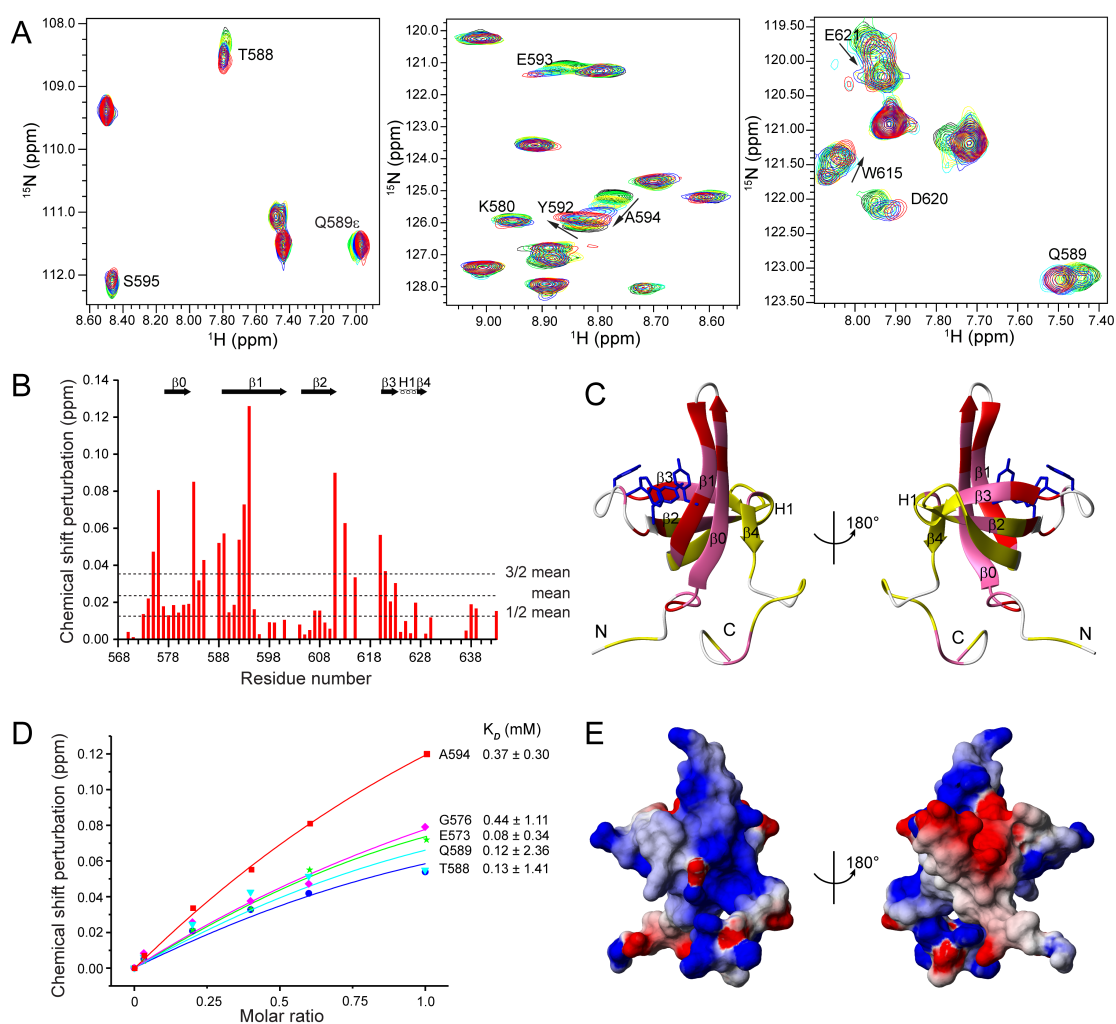


Figure S8. The interaction of RBBP1 CD and dsDNA. (A) Regions of  $^1\text{H}$ - $^{15}\text{N}$  HSQC spectra of RBBP1 CD titrated with dsDNA. (B) Bar diagram of chemical shift perturbations versus residue number at a molar ratio 1:1 of RBBP1 CD to dsDNA. (C) Mapping of chemical shift perturbations (CSP) onto the RBBP1 CD structure. The residues with a CSP value more than 1.5 times the mean CSP value are shown in red; those with a CSP value between 1.5 and 0.5 times the mean are shown in pink; and those with a CSP value less than 0.5 times the mean are shown yellow. The residues that form the aromatic cage are shown as blue sticks. (D)  $K_D$  values for binding of RBBP1 CD to dsDNA. (E) Electrostatic potential surface of RBBP1 CD. The orientations are the same as those in (C). The positively and negatively charged surfaces are in blue and red, respectively.



Figure S9.

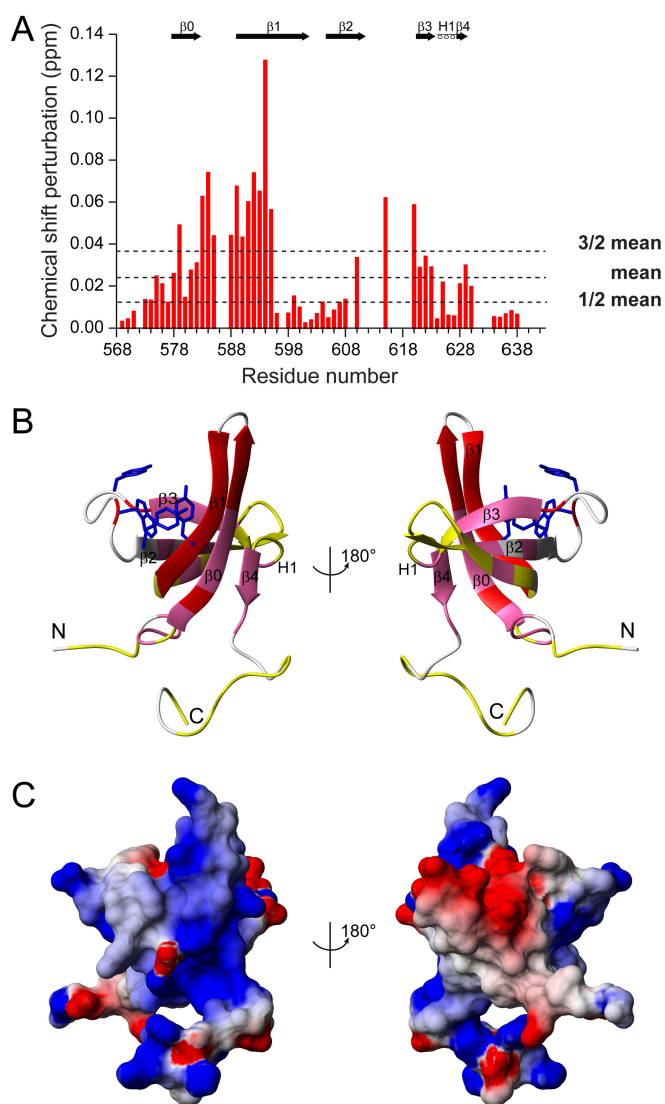


Figure S9. The interaction of the RBBP1 CD with H4K20me3 in the presence of dsDNA. (A) Bar diagram of chemical shift perturbations versus residue number at a molar ratio 1:5 of RBBP1 CD (in the presence of dsDNA at a 1:1 molar ratio to the RBBP1 CD) to H4K20me3. (B) Mapping of chemical shift perturbations (CSP) to RBBP1 CD structure. The residues with a CSP value more than 1.5 times the mean CSP value are shown in red; those with a CSP value between 1.5 and 0.5 times the mean are shown in pink; and those with a CSP value less than 0.5 times the mean are shown yellow. The residues that form the aromatic cage are shown as blue sticks. (C) Electrostatic potential surface of RBBP1 CD. The orientations are the same as those in (B). The positively and negatively charged surfaces are in blue and red, respectively.

## References

- 1 Combet, C., Blanchet, C., Geourjon, C. and Deleage, G. (2000) NPS@: network protein sequence analysis. *Trends Biochem. Sci.* **25**, 147-150
- 2 Ishida, T. and Kinoshita, K. (2007) PrDOS: prediction of disordered protein regions from amino acid sequence. *Nucleic Acids Res.* **35**, W460-464
- 3 Wu, H., Zeng, H., Lam, R., Tempel, W., Amaya, M. F., Xu, C., Dombrovski, L., Qiu, W., Wang, Y. and Min, J. Structural and Histone Binding Ability Characterizations of Human PWWP Domains. *PLoS One.* **6**, e18919
- 4 Vezzoli, A., Bonadies, N., Allen, M. D., Freund, S. M., Santiveri, C. M., Kvinlaug, B. T., Huntly, B. J., Gottgens, B. and Bycroft, M. (2010) Molecular basis of histone H3K36me3 recognition by the PWWP domain of Brpf1. *Nat. Struct. Mol. Biol.* **17**, 617-619
- 5 Krissinel, E. and Henrick, K. (2004) Secondary-structure matching (SSM), a new tool for fast protein structure alignment in three dimensions. *Acta. Crystallogr. D Biol. Crystallogr.* **60**, 2256-2268